THE JOURNAL OF BIOLOGICAL CHEMISTRY VOL. 291, NO. 23, pp. 12322–12335, June 3, 2016

Neogenin Facilitates the Induction of Hepcidin Expression by Hemojuvelin in the Liver*[S]

Received for publication, February 10, 2016, and in revised form, April 12, 2016 Published, JBC Papers in Press, April 12, 2016, DOI 10.1074/jbc.M116.721191

Ningning Zhao, Julia E. Maxson, Richard H. Zhang, Mastura Wahedi, Caroline A. Enns, and An-Sheng Zhang[1]

From the Department of Cell, Developmental, and Cancer Biology, Oregon Health & Science University, Portland, Oregon 97239

Hemojuvelin (HJV) regulates iron homeostasis by direct interaction with bone morphogenetic protein (BMP) ligands to induce hepcidin expression through the BMP signaling pathway in the liver. Crystallography studies indicate that HJV can simultaneously bind to both BMP2 and the ubiquitously expressed cell surface receptor neogenin. However, the role of the neogenin-HJV interaction in the function of HJV is unknown. Here we identify a mutation in HJV that specifically lowers its interaction with neogenin. Expression of this mutant Hjv in the liver of $Hjv^{-/-}$ mice dramatically attenuated its induction of BMP signaling and hepcidin mRNA, suggesting that interaction with neogenin is critical for the iron regulatory function of HJV. Further studies revealed that neogenin co-immunoprecipitated with ALK3, an essential type-I BMP receptor for hepatic hepcidin expression. Neogenin has also been shown to facilitate the cleavage of HJV by furin in transfected cells. Surprisingly, although cleavage of HJV by furin has been implicated in the regulation of HJV function in cell culture models and furin-cleaved soluble Hjv is detectable in the serum of mice, mutating the furin cleavage site did not alter the stimulation of hepcidin expression by Hjv in mice. *In vivo* studies validated the important role of HJV-BMP interaction for Hjv stimulation of BMP signaling and hepcidin expression. Together these data support a model in which neogenin acts as a scaffold to facilitate assembly of the HJV·BMP·BMP receptor complex to induce hepcidin expression.

Hemojuvelin (HJV for humans, and Hjv for mouse),[2] also called repulsive guidance molecule c (RGMc), is a glycosylphosphatidylinositol-linked membrane protein. It belongs to the highly conserved RGM family that also contains RGMa and RGMb. Although RGMa and RGMb are predominantly expressed in the developing and adult central nervous system and are essential for neural development (1), HJV is expressed mainly in the liver, skeletal muscle, and heart and is essential for iron homeostasis (2). Mutations in the *HJV* gene in humans markedly reduce hepcidin expression in the liver and result in juvenile hemochromatosis (JH), the most severe form of iron overload disorder (2). Hepcidin is a 25-amino acid peptide hormone that inhibits the iron efflux from enterocytes and macrophages into circulation by binding to and targeting ferroportin, the only known iron exporter, for degradation (3). It is synthesized in hepatocytes as an 84-amino acid prepropeptide that contains an N-terminal 24-amino acid signal sequence, a 35-amino acid proregion, and a C-terminal 25-amino acid bioactive peptide. After post-translational processing, the bioactive C-terminal 25-amino acid peptide is secreted into the circulation as a mature form to regulate iron homeostasis (4). Consistently, low hepatic hepcidin expression and a marked iron overload were also observed in *Hjv* knock-out ($Hjv^{-/-}$) mice (5, 6). Further studies in mice with tissue-specific *Hjv* knockdown demonstrate that only the hepatic Hjv is indispensable for hepcidin expression and iron homeostasis (7, 8).

HJV, in the liver, acts as a co-receptor for BMP6 to stimulate hepcidin expression through the BMP signaling pathway (9–11). BMP signaling is initiated upon the binding of BMP ligands to type-I and type-II BMP receptors on the cell surface. Upon BMP binding, the type-II receptors phosphorylate the type-I receptors, leading to the phosphorylation of SMAD1/5/8 in the cytoplasm. The phosphorylated SMADs form heteromeric complexes with SMAD4 and then translocate to the nucleus where they induce the transcription of target genes. HJV most likely uses two type-I BMP receptors, ALK2 and ALK3, to induce hepcidin expression, because liver-specific deletion of either *Alk3* or (to a lesser extent) *Alk2* causes iron overload in mice (12).

Structural studies of the HJV ectodomain demonstrate that it can simultaneously bind BMP2 and neogenin with nanomolar affinities through its N-terminal portion (amino acids 1–145) and C-terminal portion (amino acids 146–401), respectively, and identify the key residues in these molecules that are responsible for these interactions (13, 14). Neogenin is a ubiquitously expressed type-I transmembrane protein that contains four immunoglobulin (Ig)-like domains and six fibronectin III (FNIII) domains in its large extracellular region. HJV specifically binds to the FNIII 5–6 subdomains (15). However, the precise role of neogenin in HJV induction of hepcidin expression is still unclear, largely because of lack of an appropriate animal model. In a hepatoma cell line that expresses HJV, deprivation of neogenin abolishes BMP4 induction of hepcidin expression (16). In humans, the most common JH-causing mutation in HJV, G320V, disrupts its interaction with neogenin

* This work was supported, in whole or in part, by National Institutes of Health Grants R01DK102791 (to A. S. Z.), R01DK072166 (to C. A. E.), K99DK104066 (to N. Z.), and K99CA190605 (to J. E. M.). The content is solely the responsibility of the authors and does not necessarily represent the official views of the National Institutes of Health. The authors declare that they have no conflicts of interest with the contents of this article.

[S] This article contains supplemental Table S1 and Figs. S1–S4.

[1] To whom correspondence should be addressed: 3181 S.W. Sam Jackson Park Rd., Portland, OR 97239. Tel.: 503-494-5846; Fax: 503-494-4253; E-mail: zhanga@ohsu.edu.

[2] The abbreviations used are: HJV, hemojuvelin; RGM, repulsive guidance molecule; JH, juvenile hemochromatosis; BMP, bone morphogenetic protein; MT2, matriptase-2; HFE, hemochromatosis protein; TfR2, transferrin receptor-2; ID, iron deficient; qRT, quantitative real-time; CM, conditioned medium; FN, fibronectin.

(17). In mice, neogenin deficiency results in low hepcidin expression and severe iron overload that are indistinguishable from $Hjv^{-/-}$ mice. But interpretation of these results is complicated by other developmental defects and early death, because neogenin is also a receptor for netrins, RGMa, and RGMb (18).

Neogenin is required for the cleavage of HJV by the ubiquitously expressed furin proprotein convertases as well as matriptase-2 (MT2) in transfected cells (19, 20), and cleaved HJV is readily detectable in the conditioned medium (21–23). Furin-cleaved soluble HJV suppresses hepcidin expression in HepG2 cells (24), likely by acting as a decoy to compete with membrane HJV for BMP6. MT2 is a type II transmembrane serine protease that is predominantly expressed in hepatocytes and is a key suppressor of hepcidin expression likely by cleaving membrane HJV into inactive fragments (22, 25, 26). Although soluble HJV has been detected in the serum of humans and rats (27, 28), the role of furin-cleaved Hjv in hepatic hepcidin expression and the necessity of neogenin for the cleavage of HJV *in vivo* are still unknown.

HJV also interacts with hemochromatosis protein (HFE) and transferrin receptor-2 (TfR2) (29), which are highly expressed in hepatocytes. In humans, mutations in either HFE or TfR2 decrease hepcidin expression and cause hereditary hemochromatosis. Although the mechanisms by which HFE or TfR2 upregulate hepcidin expression has not been fully defined, a recent study indicates that HJV, HFE, and TfR2 operate in the same pathway (30). In the present study, we systemically examined the role of neogenin in Hjv-mediated induction of hepcidin expression in the liver of mice. Results demonstrate that an efficient induction of hepcidin expression by Hjv requires its interaction with neogenin.

Experimental Procedures

cDNA Constructs—We generated mouse Hjv ORF in pGEM-T vector (Hjv-pGEM-T) in our previous study (31). Hjv with a glycine to valine substitution at amino acid 92 (G92V-Hjv; Table 1) was generated by site-directed mutagenesis using the QuikChange kit (Stratagene). After verification by sequencing, both Hjv and G92V-Hjv constructs were subcloned into an AAV8 construct containing a strong liver-specific promoter as described in our previous study (31). The liver-specific promoter is a combination of two copies of a human α1-microglobulin/bikunin enhancer and the promoter from the human thyroid hormone-binding globulin gene.

We generated a FLAG-tagged Hjv construct using the same strategy as described for human HJV (9). Briefly, the Hjv coding sequence without the signal peptide was amplified from Hjv-pGEM-T by PCR using the Expand High Fidelity PCR System (Roche Applied Science, Indianapolis, IN), followed by cloning into p3XFLAG-CMV9 (Sigma) downstream of the preprotrypsin signal sequence and FLAG tag (fHjv-pCMV9). Hjv coding sequence with alanine to arginine substitution at amino acid 183 (A183R-fHjv), arginine to alanine substitution at amino acid 281 (R281A-fHjv), arginine to alanine substitution at amino acid 325 (R325A-fHjv), and glycine to valine substitution at amino acid 313 (G313V-fHjv) were generated from fHjv by site-directed mutagenesis. fHjv, A183R-fHjv, R281A-fHjv, R325A-fHjv, and G313V-fHjv sequences were subcloned into an AAV8 construct as described above for Hjv. All mutations were verified by DNA sequencing.

pCMV9 vector containing human HJV coding sequence with a N-terminal FLAG tag (fHJV-pCMV9) were obtained from Dr. Jodie Babitt and Dr. Herbert Lin, Massachusetts General Hospital (9). cDNAs encoding mutant HJV with glycine to valine substitution at amino acid 99 (G99V-fHJV), alanine to arginine substitution at amino acid 190 (A190R-fHJV), arginine to alanine substitution at amino acid 288 (R288A-fHJV), arginine to alanine substitution at amino acid 332 (R332A-fHJV), and glycine to valine substitution at amino acid 320 (G320V-fHJV) were generated from fHJV-pCMV9 by site-directed mutagenesis. All mutations were verified by DNA sequencing.

Human neogenin ORF with a C-terminal VSG-G tag in pcDNA3.1 (pcDNA3-neogenin) were obtained from Dr. Eric R. Fearon at the University of Michigan Medical School, Ann Arbor, MI. We generated a truncated neogenin construct with a deletion of Ig 1–4 domains but still retaining an intact signal sequence (neogenin/ΔIg) by PCR using site-directed mutagenesis and the following primers: 5′-gggcgccgggcgccgcg**gcgcct**tcagctcctcgggatgt-3′ (forward) and 5′-acatcccgaggagctgaaggcgccgcggcgcccggcgccc-3′ (reverse). The sequence was verified by DNA sequencing. We obtained human ALK2 ORF with an HA tag in pcDNA3 (pcDNA3-ALK2/HA) and human ALK3 ORF with an HA tag in pcDNA3 (pcDNA3-ALK3/HA) from Dr. Peter ten Dijke (Leiden University, The Netherlands).

Animal Analysis—$Hjv^{-/-}$ mice on the 129/SvEvTac (129/S) background were obtained from Dr. Nancy Andrews (Duke University). Both $Hjv^{-/-}$ and wild-type 129/S mice were bred and maintained in the Oregon Health and Science University DCM. We performed three separate sets of studies with at least 5 animals for each group.

For the first study, 8-week-old male $Hjv^{-/-}$ mice were intraperitoneally injected with PBS, AAV8-fHjv, A183R-fHjv, or G313V-fHjv at $\sim 5 \times 10^{11}$ and/or $\sim 10^{13}$ genome-particles per mouse. Three weeks later, mice were euthanized for analysis. Blood was collected by cardiac puncture for serum iron and Hjv analysis. Livers were rapidly removed, snap-frozen in liquid nitrogen, and then stored at −80 °C for qRT-PCR, Western blotting, immunoprecipitation, and tissue nonheme iron assays. Age and gender-matched wild-type and $Hjv^{-/-}$ mice were included as additional controls.

For the second study, male $Hjv^{-/-}$ mice were fed an iron-deficient (ID) diet (less than 1 ppm iron, TestDiet, Richmond, IN; low iron group) starting from 5 weeks old until euthanization to deplete bodily iron stores. Animals at the age of 8 weeks old were intraperitoneally injected with PBS, $\sim 5 \times 10^{11}$ AAV8-fHjv, R281A-fHjv, R325A-fHjv, or GFP genome-particles per mouse. Three weeks later, mice were euthanized for analysis as described above. At 4, 16, and 24 h before euthanization, mice in AAV8-fHjv, R281A-fHjv, and R325A-fHjv groups were intraperitoneally injected with aprotinin (G Biosciences) at ~80 mg/kg body weight in PBS or with the vehicle only.

The third study for G92V-Hjv was performed in the same setting as in our previous report for Hjv (31). Briefly, 8-week-old male $Hjv^{-/-}$ mice were injected with $\sim 5 \times 10^{11}$ AAV8-Hjv or G92V-Hjv vector particles per mouse via the tail vein. Two

weeks later, mice were euthanized for analysis. All procedures for animal use were approved by the Oregon Health and Science University DCM. The viral vector stocks were handled according to Biohazard Safety Level 2 guidelines published by the National Institutes of Health.

Quantitative Real-time RT-PCR (qRT-PCR)—qRT-PCR analysis of β-actin, Activin-B, Bmp6, hepcidin, Hjv, Id1, and IL-6 transcripts in the liver were conducted as previously described (31). The mouse primers used for qRT-PCR are listed in supplemental Table S1. All primers were verified for linearity of amplification. The results are expressed as the amount relative to that of β-actin for each sample.

Serum Iron and the Liver Nonheme Iron Assays—Serum iron concentrations were measured using a serum iron/TIBC Reagent Set (Teco Diagnostics, Anaheim, CA). Nonheme iron concentrations in the liver tissues were determined as described in our previous studies (31).

Immunodetection of fHjv and Smad Proteins in Mice—Liver extracts were separated using SDS-PAGE, probed with mouse anti-FLAG M2 IgG (1:10,000; Sigma), rabbit anti-phosphorylated Smad1/5/8 (pSmad, 1:1,000; Cell Signaling Technology), rabbit anti-Smad1/5/8 (Smad, 1:500; Santa Cruz), and mouse anti-β-actin (1:10,000; Sigma), and immunodetected by using an Alexa Fluor 680 goat anti-rabbit secondary antibody or an Alexa Fluor 800 goat anti-mouse secondary antibody. Images were visualized and quantified using an Odyssey Infrared Imaging System (Licor). Additionally, fHjv in the liver extracts was also detected directly by using an HRP-coupled mouse anti-FLAG M2 IgG (1:10,000; Sigma) and chemiluminescence (Super Signal, Pierce) to reduce the nonspecific background. For immunodetection of serum fHjv, fHjv in ~60 μl of serum was pulled down with mouse anti-FLAG M2 beads (Sigma), followed by elution using 1× Laemmli buffer, separation using SDS-PAGE, and immunodetection using HRP-coupled mouse anti-FLAG M2 IgG and chemiluminescence. The intensities of fHjv bands in x-ray films were quantified by using ImageJ software.

Immunoprecipitation—We used HeLa cells that stably express both human TfR2 and HFE with a C-terminal FLAG tag (HeLa-TfR2/fHFE) for co-immunoprecipitation analysis of human HJV and mutants with TfR2 and HFE. Briefly, HeLa-TfR2/fHFE cells were transiently transfected by pcDNA3 empty vector, pcDNA3-HJV, and mutants using TransIt-2020 transfection reagent (Mirus). After 48 h of transfection, cell lysates were prepared using NET-Triton buffer with 1× Protease inhibitors mixture. Cell lysate was first incubated with protein A-agarose beads for 30 min to pre-clear the nonspecific binding. Immunoprecipitation was performed using protein A-agarose beads (Invitrogen) and rabbit anti-HJV 18745 antibody (generated against residues 1–401 of human HJV). Immunoprecipitated proteins bound to protein A-agarose beads were washed, eluted, separated by SDS-PAGE, and transferred to a nitrocellulose membrane. Membranes were probed with mouse anti-TfR2, HJV, or FLAG antibody, followed by immunodetection using an Alexa Fluor 800 goat anti-mouse secondary antibody and visualized using a Licor.

We used HEK293 cells that stably express the transfected human neogenin (HEK293-neogenin) for the immunoprecipitation analysis with human HJV and their mutants, and HEK293 cells for the immunoprecipitation analysis with murine Hjv and their mutants. Briefly, HEK293-neogenin cells were transiently transfected by pcDNA3 empty vector, pcDNA3-HJV, and mutants using TransIt-2020 transfection reagent. HEK293 cells were co-transfected by pcDNA3-neogenin with pcDNA3 empty vector, pCMV9-fHjv, or mutants. After 48 h of transfection, immunoprecipitation was performed using protein A-agarose beads and rabbit anti-HJV 18745 antibody for human HJV and anti-FLAG M2 beads for murine fHjv as described above. Immunoprecipitated proteins were probed with mouse anti-HJV, goat anti-neogenin (C20; Santa Cruz), or mouse anti-FLAG antibody, followed by immunodetection using an Alexa Fluor 800 goat anti-mouse secondary antibody or an Alexa Fluor 680 donkey anti-goat secondary antibody and visualized using a Licor.

We used HEK293 cells that stably express ALK2/HA or ALK3/HA (HEK293-ALK2/HA or ALK3/HA) for the immunoprecipitation analysis with neogenin and neogenin/ΔIg. Briefly, HEK293-ALK2/HA and ALK3/HA cells were transiently transfected by pcDNA3 empty vector, pcDNA3-neogenin, and pcDNA3-neogenin/ΔIg plasmid DNA using TransIt-2020 transfection reagent. After 48 h of transfection, cell lysates were prepared. Immunoprecipitation was performed using protein A-agarose beads and rabbit anti-neogenin FNIII 1–6 as described above. Immunoprecipitated proteins were probed with mouse anti-HA (12CA5; Abcam), goat anti-neogenin (C20; Santa Cruz), or mouse anti-β-actin antibody, followed by immunodetection using an Alexa Fluor 800 goat anti-mouse secondary antibody or an Alexa Fluor 680 donkey anti-goat secondary antibody and visualized using a Licor.

We used liver extracts from $Hjv^{-/-}$ mice injected with AAV8-fHjv, A183R-fHjv, and G313V-fHjv vectors at $\sim 5 \times 10^{11}$ genome particles per mouse for the co-immunoprecipitation analysis with neogenin *in vivo*. Briefly, about 3 mg of extract protein was immunoprecipitated by using anti-FLAG M2 beads for fHjv as described above. The immunoprecipitated proteins and about 250 μg of extract protein (input) were subjected to SDS-PAGE, followed by immunodetection using a HRP-coupled mouse anti-FLAG M2 IgG and chemiluminescence for fHjv and using a rabbit anti-neogenin FNIII 1–6, an Alexa Fluor 680 goat anti-rabbit secondary antibody, and a Licor for neogenin.

Biotinylation of Cell Surface Proteins—HEK293 cells were plated in the polylysine-coated 6-well plate and transfected with pcDNA3 empty vector, pcDNA3-fHjv, A183R-fHjv, G313V-fHjv, neogenin and neogenin/ΔIg plasmid DNA using Lipofectamine 2000 (Invitrogen). After 48 h of transfection, cell surface proteins were biotinylated with 0.25 mg/ml of Sulfo-NHS-Biotin (Thermo Fisher Scientific) at 4 °C for 30 min. After the reaction was terminated, cells were immediately solubilized in NET-Triton, 1× protease inhibitors mixture (Roche Applied Science). Biotinylated proteins were isolated using streptavidin-agarose beads (Thermo Fisher Scientific). Bound proteins were eluted with NET-Triton, 1× Laemmli buffer, subjected to SDS-PAGE, probed with mouse anti-HJV, mouse anti-Na^+/K^+-ATPase α1 (Santa Cruz), rabbit anti-neogenin FNIII 1–6, or mouse anti-β-actin antibody, and immunodetected using an

Alexa Fluor 800 goat anti-mouse secondary antibody or an Alexa Fluor 680 goat anti-rabbit secondary antibody and visualized using a Licor.

Analysis of HJV Secretion—HepG2 cells that stably expressed HJV (HepG2-HJV) were plated in 12-well plates. After 2 days of incubation, fresh medium (MEM, 10% FCS) containing various concentrations of aprotinin (0, 0.005, 0.01, 0.05, 1, 5, and 10 μM) was replaced, and cell lysate and conditioned medium (CM) cells were collected after an additional 16 h of incubation. About 50% of cell lysate and 10% of CM were subjected to SDS-PAGE and immunodetection using rabbit anti-HJV antibody, HRP-conjugated goat anti-rabbit secondary antibody, and chemiluminescence.

Statistical Analysis—One-way analysis of variance and Tukey's post test were used to compare three or more sets of data. Only the results for the groups of interest were presented.

TABLE 1
Mutations in HJV used in this study
The wild-type amino acid is listed first and the mutant is listed last.

Human residue	Eq. murine residue	Disrupted interaction/function	References
G99V	G92V	BMP2	33
A190R	A183R	Neogenin	This study
R288A	R281A	Neogenin	This study
		MT2 cleavage	24
G320V	G313V	Neogenin	17
R332A	R325A	Furin cleavage	24

Results

Identification of a Mutation in HJV That Disrupts Its Interaction with Neogenin, but Not TfR2 or HFE—To determine the role of the HJV·neogenin complex in the induction of hepcidin expression *in vivo* we generated a new mutant form of HJV that fails to interact with neogenin. G320V-HJV (corresponding to G313V-Hjv in mouse; Table 1) that does not interact with neogenin (17) is not ideal because of the contradictory results of its cell surface localization in previous studies (32, 33). Based on the crystallographic and binding studies, Ala-186 is a key highly conserved residue involved in the interaction of the closely related RGMb with neogenin (14). In human HJV the equivalent residue is Ala-190 and in murine Hjv it is Ala-183. We tested whether mutations in this site in human HJV (A190R-HJV; Fig. 1*A*) and in mouse Hjv (A183R-fHjv, Fig. 1*B*) could disrupt interaction with neogenin. For mouse Hjv a construct

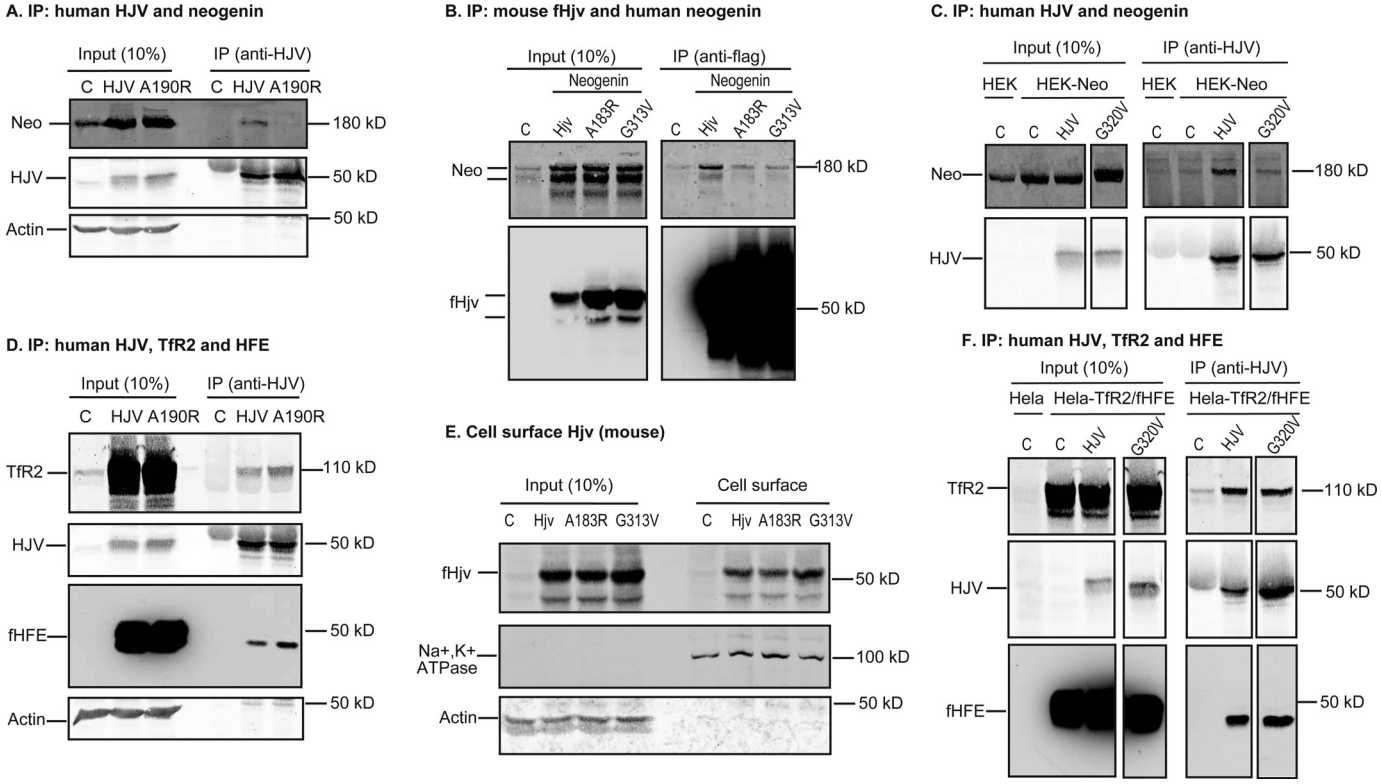

FIGURE 1. **Interaction of mutant hemojuvelin with neogenin and cell surface localization of Hjv.** *A,* A190R-HJV did not co-immunoprecipitate with neogenin. HEK293-neogenin cells were transfected by pcDNA3 (*C*), pcDNA3-HJV or A190R-HJV, immunoprecipitated (*IP*) by using anti-HJV antibody generated against residues 1–401 of HJV, and immunodetected for neogenin (*Neo*), HJV, and β-actin. *B,* co-immunoprecipitation of WT and mutant fHjv with neogenin. HEK293 cells were co-transfected by pcDNA3-neogenin with pCMV9-fHjv, A183R-fHjv, or G313V-fHjv, immunoprecipitated by using anti-FLAG M2 beads, and immunodetected for neogenin (*Neo*) and fHjv. HEK293 cells transfected with pCMV9 alone (*C*) were included as a control. The entire images are illustrated in supplemental Fig. S1*A*. *C,* co-immunoprecipitation of WT and mutant HJV with neogenin. HEK293-neogenin (HEK-Neo) cells were transfected by pcDNA3 (*C*), pcDNA3-HJV, and G320V-HJV, immunoprecipitated by using anti-HJV antibody, and immunodetected for neogenin (*Neo*) and HJV. HEK293 cells (HEK) were included as a control. The entire images are illustrated in supplemental Fig. S1*B*. *D,* co-immunoprecipitation of WT and A190R-HJV with HFE and TfR2. HeLa-TfR2/fHFE cells were transfected by pcDNA3 (*C*), pcDNA3-HJV, and A190R-HJV, immunoprecipitated by using anti-HJV antibody, and immunodetected for TfR2, HJV, and fHFE. *E,* biotinylation of cell surface Hjv. HEK293 cells were transfected with pCMV9 (*C*), pCMV9-fHjv, A183R-fHjv, and G313V-fHjv, followed by biotinylation of cell surface proteins at 4 °C. fHjv, Na^+/K^+-ATPase, and β-actin in the biotinylated proteins (*Cell surface*) and cell lysate input (*Input*) were immunodetected. *F,* co-immunoprecipitation of WT and G320V-HJV with HFE and TfR2. HeLa-TfR2/fHFE cells were transfected by pcDNA3 (*C*), pcDNA3-HJV, and G320V-HJV, immunoprecipitated by using anti-HJV antibody, and immunodetected for TfR2, HJV, and fHFE. The entire images are illustrated in supplemental Fig. S1*C*. All experiments were repeated at least three times with consistent results.

with a 3× FLAG sequence at the site immediately after the signal peptide was used because the FLAG tag was necessary for detection of Hjv in subsequent *in vivo* experiments. A190R-HJV, A183R-fHjv, and wild-type counterparts were transfected into HEK293 cells that express endogenous and transfected neogenin. Both A190R-HJV and A183R-fHjv had reduced interaction with human neogenin as judged by co-immunoprecipitation using anti-HJV or anti-FLAG antibody, respectively (Fig. 1, *A* and *B,* and supplemental Fig. S1*A*). As positive controls, both HJV and fHjv were able to pulldown neogenin (Fig. 1, *A* and *B*). As negative controls, both G320V-HJV and G313V-fHjv had decreased interaction with neogenin by co-immunoprecipitation (Fig. 1, *B* and *C,* supplemental Fig. S1, *A* and *B*). These results confirmed Ala-190 in HJV or Ala-183 in Hjv as key residues for a high affinity interaction with neogenin, mutation of which could serve as a new tool for interrogating the importance of the HJV-neogenin interaction *in vivo*.

We next examined the effect of the A190R mutation in HJV on the interaction with TfR2 and HFE. To avoid the potential effects of sequence difference between species, only human proteins were used. HeLa cells that express TfR2 and FLAG-tagged HFE (HeLa-TfR2/fHFE) were transfected with HJV or mutants. Similar to wild-type HJV, A190R-HJV was co-immunoprecipitated with TfR2 and fHFE using anti-HJV antibody (Fig. 1*D*). These results indicate that disruption of the HJV-neogenin interaction does not affect HJV interaction with TfR2 or HFE. Additionally, the A183R mutation did not reduce fHjv localization on the plasma membrane in HEK293 cells by biotinylation of cell surface proteins (Fig. 1*E*). These results indicate that disruption of the HJV·neogenin complex does not affect either HJV interaction with TfR2 and HFE or its cell surface localization, making A183R-Hjv a good tool for assessing the importance of the Hjv-neogenin interaction *in vivo*. Interestingly, similar results were also obtained for G320V-HJV and G313V-fHjv (Fig. 1, *E* and *F*, and supplemental Fig. S1*C*). Thus G313V-fHjv is also a good candidate for *in vivo* studies.

Disruption of Hjv·Neogenin Complex Attenuates Hjv Induction of Hepcidin mRNA in the Liver of $Hjv^{-/-}$ Mice—To determine the *in vivo* role of the Hjv-neogenin interaction, we established an animal model to express fHjv in the liver of $Hjv^{-/-}$ mice using an AAV8 vector. Our previous studies indicate that AAV8 with a liver-specific promoter limits Hjv expression specifically to the liver and does not induce inflammation that could complicate interpretation of the results (31). Addition of a 3xFLAG tag to Hjv was used to detect Hjv in mouse tissues and serum, because in our hands there was no available antibody to detect Hjv *in vivo*. fHjv, A183R-fHjv, or G313V-fHjv in AAV8 ($\sim 5 \times 10^{11}$ genome particles per mouse) were intraperitoneally administered into 8-week-old male $Hjv^{-/-}$ mice fed a regular diet. Animals were euthanized for analysis 3 weeks after injection. The mRNA levels of fHjv, A183R-fHjv, and G313V-fHjv in the liver were comparable with that of wild-type mice (Fig. 2*A*). Consistently, Western blotting analysis using anti-FLAG antibody detected similar levels of fHjv and A183R-fHjv, and about 50% higher level of G313V-fHjv, which migrated at ~55 kDa and corresponded to the expected full-length Hjv (Fig. 2, *B, top panels, lanes 5–8, 11*, and *12*, and *C*). As negative controls, no corresponding band was detected either in wild-type mice or in $Hjv^{-/-}$ mice (Fig. 2, *B* and *C*). In line with our previous studies using Hjv with no tag (31), expression of fHjv was able to fully correct the low hepcidin status in $Hjv^{-/-}$ mice, and the level of hepcidin mRNA was even greater than that of wild-type mice (Fig. 2*D*). The levels of hepatic hepcidin mRNA were used as an indicator for the levels of serum hepcidin throughout the animal studies, because recent studies demonstrated a strong correlation between the levels of hepatic hepcidin mRNA and serum hepcidin in mice (34–36). The increased hepcidin mRNA was associated with an increase in phosphorylated Smad1/5/8 (pSmad) and the mRNA level of Id1 (Fig. 2, *B* and *E,* and supplemental Fig. S2*A*), consistent with the idea that fHjv induces hepcidin expression by activating the BMP signaling pathway. The phosphorylation of Smad1/5/8 is a direct indicator of the activation of BMP signaling, whereas Id1 is a direct target of BMP signaling. Both IL-6 and Activin-B are inflammatory factors that can induce hepcidin expression through Stat3 and the BMP signaling pathway, respectively, independent of Hjv (37). There was no significant change in either IL-6 or Activin-B mRNA levels in the livers (supplemental Fig. S2, *B* and *C*). Thus expression of fHjv in the liver was able to specifically induce hepcidin expression, which was correlated with stimulation of the BMP signaling. Consistent with the role of hepcidin in the suppression of iron efflux from enterocytes and macrophages, induction of hepcidin expression by fHjv significantly decreased the levels of both serum iron and the liver non-heme iron (Fig. 2, *F* and *G*). The latter is an indicator of bodily iron stores.

Expression of a similar level of A183R-fHjv in mouse livers to that of fHjv (Fig. 2*B, lanes 7* and *8 versus 5* and *6*, and *C*) was only able to mildly increase hepcidin mRNA (Fig. 2*D*). As a negative control, expression of a comparable level of G313V-fHjv, a mutant form of Hjv that causes JH, also exhibited a similarly attenuated induction of hepcidin expression (Fig. 2, *A–D*). In contrast to fHjv, neither A183R-fHjv nor G313V-fHjv was able to significantly increase the levels of pSmad1/5/8 (Fig. 2*B, lanes 7/8* and *11/12 versus 5/6*, supplemental Fig. S2*A*) and Id1 mRNA (Fig. 2*E*). Both Smad1/5/8 and β-actin were included as loading controls (Fig. 2*B*). These results indicate that the decreased hepcidin induction by A183R or G313V-fHjv resulted from lack of stimulation of BMP signaling in the liver. In agreement with low hepcidin mRNA, expression of neither A183R-Hjv nor G313V-fHjv was able to lower the levels of serum iron and liver non-heme iron (Fig. 2, *F* and *G*). Consistent with the findings in transfected cells, both A183R-fHjv and G313V-fHjv exhibited reduced interaction with neogenin in the liver extracts by co-immunoprecipitation using anti-FLAG antibody, when compared with fHjv (Fig. 2*H*). These results indicate that disruption of Hjv-neogenin interaction markedly reduces Hjv induction of hepcidin expression in the liver.

To test whether increased expression of fHjv mutants could correct the status of low hepcidin expression, $Hjv^{-/-}$ mice were intraperitoneally administered a 20-fold higher dose of AAV8-A183R-fHjv and G313V-fHjv. The levels of hepatic Hjv mRNA in A183R-fHjv and G313V-fHjv groups reached about 25- and 16.5-fold higher than that of fHjv group, respectively (Fig. 2*A*). The protein levels of A183R and G313V-fHjv in the liver were similarly increased (Fig. 2, *B, lanes 9/10* and *13/14*, and *C*).

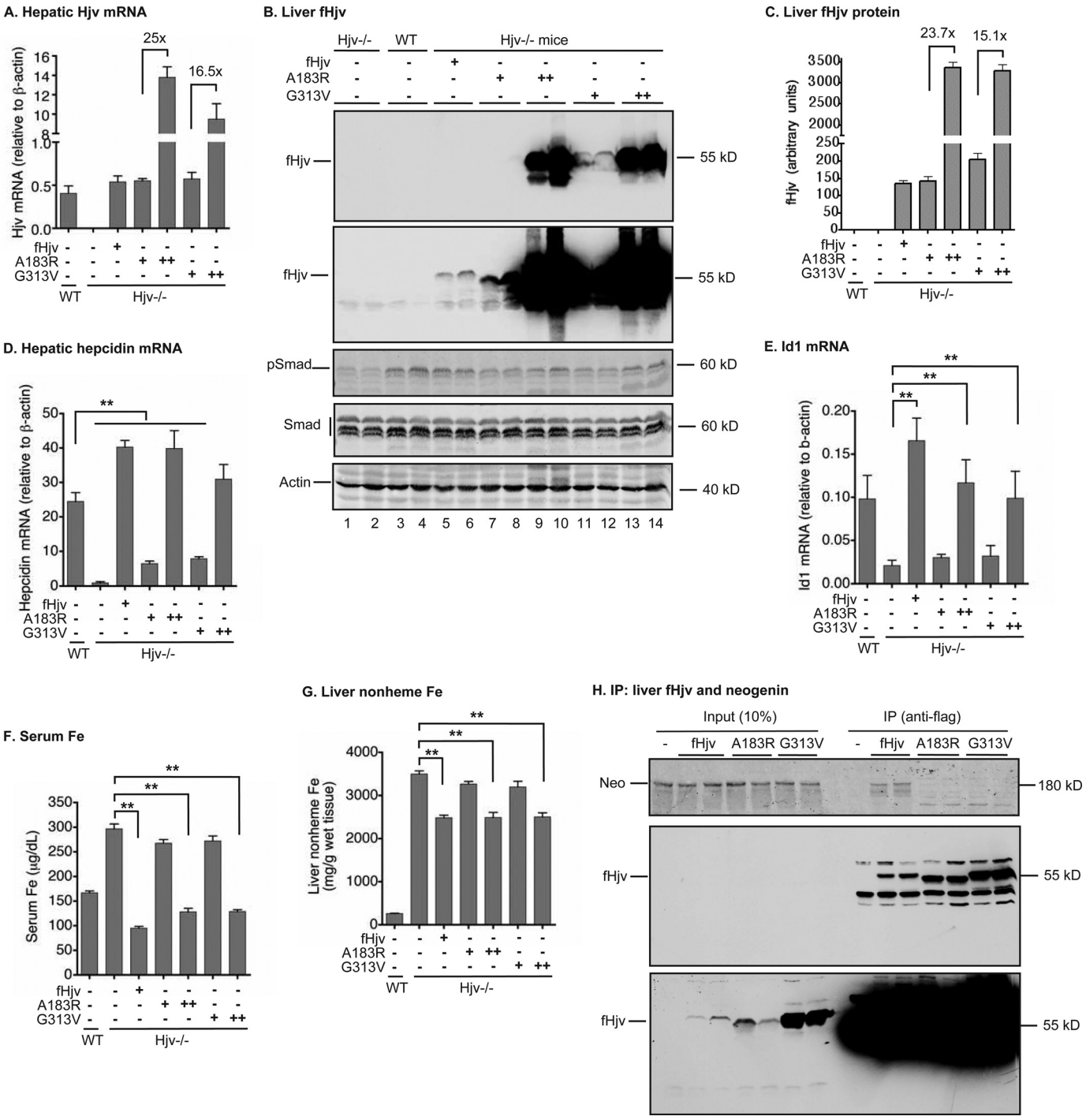

FIGURE 2. **Both A183R and G313V-fHjv had a reduced ability to induce the BMP signaling and hepcidin expression in Hjv$^{-/-}$ mice.** Eight-week-old male *Hjv*$^{-/-}$ mice were intraperitoneally injected with AAV8-fHjv, A183R-fHjv, or G313V-fHjv at ~5×10^{11} (+) and/or ~10^{13} (++) genome-particles per mouse. Age and gender-matched WT and *Hjv*$^{-/-}$ mice were included as controls. *A,* qRT-PCR analysis of Hjv mRNA in the liver. *B,* Western blot analysis of fHjv, pSmad1/5/8 (pSmad), total Smad1/5/8 (Smad), and β-actin in 150 μg of liver extracts from two mice for each condition. *C,* quantification of fHjv bands in the Western blot images of liver extracts by Licor. *D* and *E,* qRT-PCR analysis of hepcidin and Id1 mRNA in the liver. *F,* serum iron analysis. *G,* liver nonheme iron analysis. *H,* co-immunoprecipitation of fHjv with neogenin in the liver. About 3 mg of liver extract protein from *Hjv*$^{-/-}$ mice injected with AAV8-fHjv, A183R-fHjv, and G313V-fHjv vectors at ~5×10^{11} genome particles per mouse was immunoprecipitated by using anti-FLAG M2 beads for fHjv, and immunodetected for fHjv and neogenin by using HRP-coupled mouse anti-FLAG M2 IgG and rabbit anti-neogenin FNIII 1–6 antibody, respectively. About 250 μg of extract protein for each sample was loaded as input. For all qRT-PCR analysis, the results are expressed as the amount relative to that of β-actin for each sample. The mean ± S.D. are presented. $n = 5$ for each group. **, $p < 0.01$.

Interestingly, overexpression of these mutants was able to increase hepatic hepcidin mRNA to a level similar to the mice with wild-type fHjv (Fig. 2*D*). Consistently, elevated hepcidin mRNA was correlated with increases in pSmad (Fig. 2, *B, lanes 9*/*10* and *13*/*14*, supplemental Fig. S2*A*) and Id1 mRNA (Fig. 2*E*). Importantly, injection of a large amount of AAV8 did not induce any evident inflammation as measured by a lack of increase in IL-6 and Activin-B mRNA in the liver (supplemental

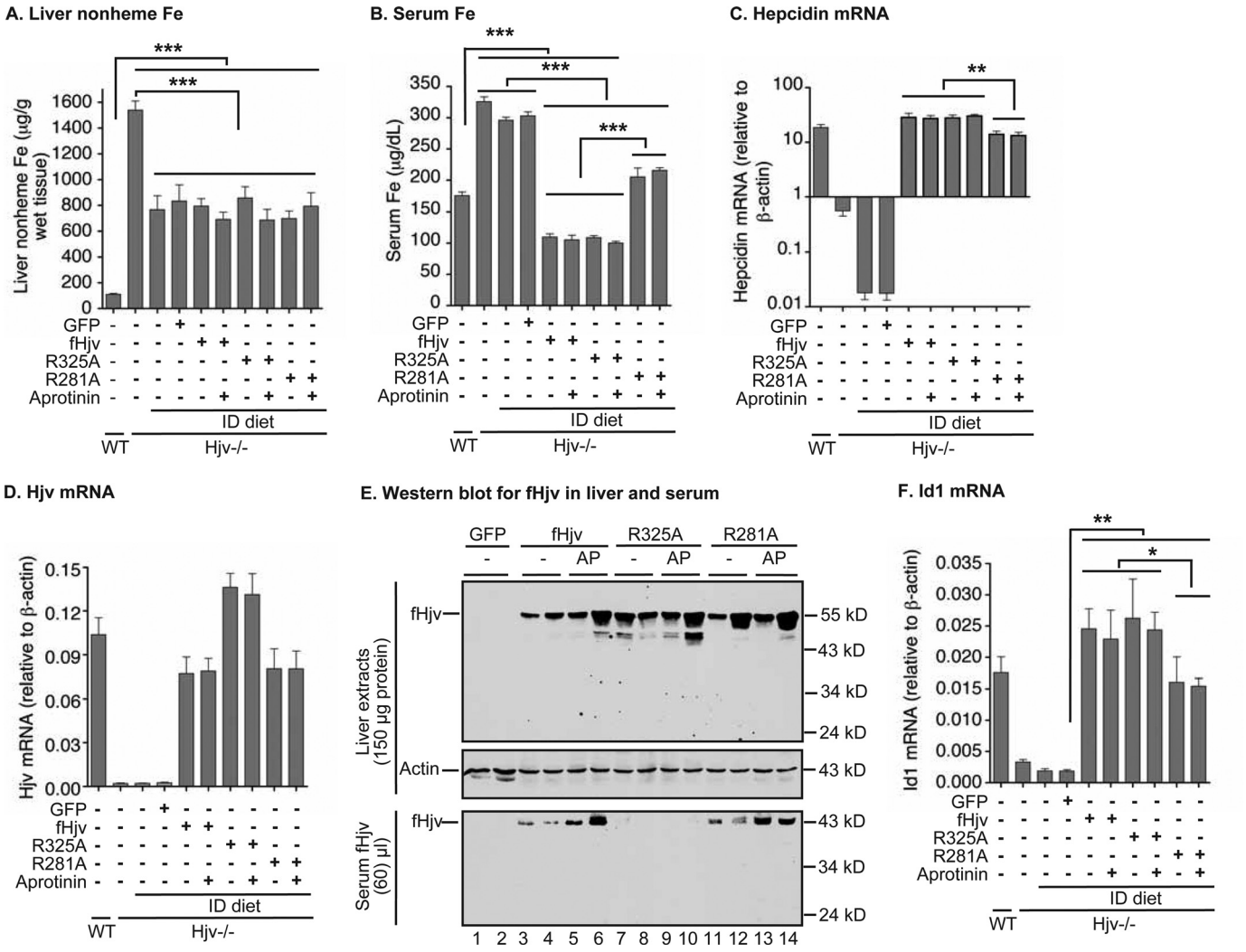

FIGURE 3. **Furin and MT2 cleavage of fHjv, R325A-fHjv, and R281A-fHjv and the induction of hepcidin expression in the liver of $Hjv^{-/-}$ mice.** Eight-week-old male $Hjv^{-/-}$ mice fed an ID diet were intraperitoneally injected with PBS, AAV8-fHjv, R281A-fHjv, R325A-fHjv, or GFP at $\sim 5 \times 10^{11}$ genome particles per mouse, and with aprotinin before euthanization. Age and gender-matched WT and $Hjv^{-/-}$ mice fed a regular diet were included as additional controls. *A,* liver nonheme iron analysis. *B,* serum iron analysis. *C* and *D,* qRT-PCR analysis of hepcidin and Hjv mRNA in the liver. *E,* Western blot analysis of fHjv and β-actin in 150 μg of liver extracts and fHjv in 60 μl of serum from two mice for each condition. *AP*, aprotinin. *F,* qRT-PCR analysis of Id1 mRNA in the liver. All qRT-PCR results are expressed as the amount relative to that of β-actin for each sample. The mean ± S.D. are presented. $n = 5$ for each group. *, $p < 0.05$; **, $p < 0.01$; ***, $p < 0.001$.

Fig. S2, *B* and *C*). As expected, increased hepcidin mRNA led to a significant reduction of serum iron and the liver non-heme iron (Fig. 2, *F* and *G*). These results indicate that both A183R and G313V-fHjv are partially functional and in excess can induce hepcidin expression through the BMP signaling pathway. At physiological levels, however, the inability to interact with neogenin prevents these Hjv mutants from properly controlling iron levels through regulation of hepcidin expression.

Interaction with Neogenin Is Not Required for Furin Cleavage of Hjv in Vivo and Abolishment of Furin Cleavage in Hjv Does Not Affect the Induction of Hepatic Hepcidin mRNA—The cleavage of HJV by furin is promoted by neogenin in cell culture models, and furin-cleaved soluble HJV is proposed to suppress the function of membrane HJV. The essential furin cleavage site in HJV was mapped to Ala-332 (corresponding to Ala-325 for mouse Hjv) at the conserved polybasic RNRR motif, and the R332A mutation in HJV abolishes furin cleavage in cultured cells (21, 23, 24). To determine whether neogenin regulates the cleavage *in vivo* and the role of furin-cleaved Hjv in hepatic hepcidin expression, both fHjv and R325A-fHjv were expressed in the livers of $Hjv^{-/-}$ mice. Expression of AAV8-GFP was included as a negative control. Mice were fed an ID diet starting from 5 weeks of age to deplete excess liver iron. In cellular studies, furin cleavage of HJV is negatively regulated by iron (21, 23, 28). $Hjv^{-/-}$ mice fed an ID diet for 6 weeks led to decreased liver non-heme iron by about 50%, serum iron by ~10%, and hepatic hepcidin mRNA by about 100-fold compared with $Hjv^{-/-}$ mice fed a regular iron diet (Fig. 3, *A–C*). Consistent with the finding that BMP6 mRNA levels are positively regulated by iron in the liver (38), hepatic BMP6 mRNA levels decreased by about 50% (supplemental Fig. 3*A*). Hjv mRNA levels for both fHjv and G325A-fHjv groups were comparable with those of wild-type mice (Fig. 3*D*). Western blotting analysis revealed similar levels of fHjv and G325A-fHjv in the liver extracts (Fig. 3*E, top panel, and lanes 3/4 versus 7/8,* supplemental Fig. S3*B*). To detect the furin-cleaved fHjv, ~60

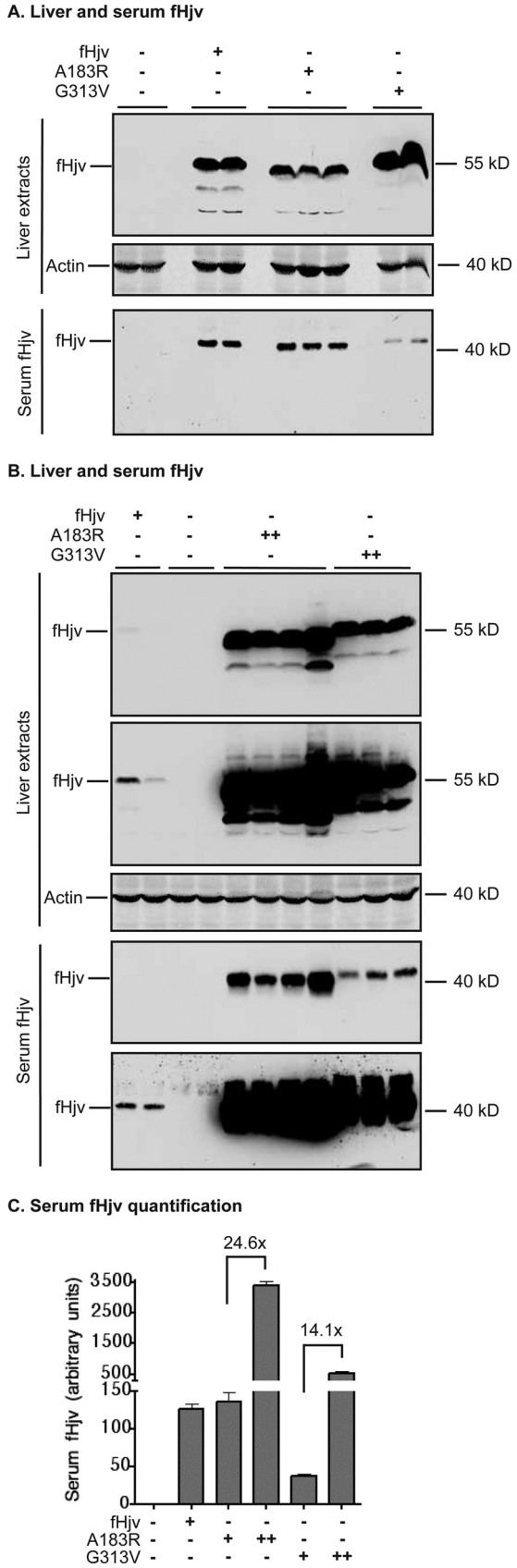

FIGURE 4. **Secretion of furin-cleaved fHjv, A183R-fHjv, and G313V-fHjv from liver into the circulation.** Eight-week-old male *Hjv*$^{-/-}$ mice were intraperitoneally injected with AAV8-fHjv, A183R-fHjv, or G313V-fHjv at ~5 × 10^{11} (+) and ~10^{13} (++) genome particles per mouse as described in the legend to Fig. 2. *A* and *B*, Western blotting analysis of fHjv and β-actin in 150 μg of liver extracts and soluble fHjv in 60 μl of serum. Two images for both liver extract and serum fHjv with different exposures were presented in *B*. *C*, quantification of serum fHjv bands in Western blot images by ImageJ software ($n = 5$).

μl of serum was immunoprecipitated with anti-FLAG beads, followed by immunodetection using HRP-conjugated anti-FLAG IgG. A single distinct fHjv band migrating at ~43 kDa was observed in the serum of fHjv mice but not in GFP mice (Fig. 3*E, lower panel, lanes 3* and *4*). The molecular weight corresponds to that of the predicted size of the furin-cleaved product. In contrast, no serum fHjv was detected in the serum of R325A-fHjv mice (Fig. 3*E, lower panel*, *lanes 7* and *8*). These findings indicate that furin uses the same site to cleave Hjv in the liver as in transfected cells.

To test the role of neogenin in furin cleavage of Hjv, we compared the relative levels of serum fHjv in *Hjv*$^{-/-}$ mice expressing fHjv, to the A183R, and G313V mutants that have reduced interaction with neogenin. The sizes of serum Hjv from all three groups corresponded to the furin-cleaved products (Fig. 4, *A* and *B*). When comparable levels of fHjv protein were expressed in the liver, we detected similar levels of serum fHjv between fHjv and A183R-fHjv groups, and a relatively low level in the G313V-fHjv group (Fig. 4*A, lower panel*). Interestingly, when the levels of A183R and G313V-fHjv proteins were increased in the liver, serum fHjv levels from both groups were proportionally increased (Figs. 2, *B* and *C*, and 4, *B* and *C*), indicating that mutated proteins were able to be processed and secreted. These results suggest that interaction with neogenin is not required for furin cleavage of Hjv in the liver.

Because furin-mediated cleavage of HJV negatively regulates HJV activity in the human hepatoma cell line HepG2 cells (24), we compared hepcidin expression in fHjv mice to that of R325A-fHjv mice to determine whether soluble Hjv inhibits hepcidin expression *in vivo*. Expression of fHjv in the liver of *Hjv*$^{-/-}$ mice was able to robustly increase hepcidin mRNA by about 1000-fold, reaching a level well above that of wild-type mice (Fig. 3*C*). As a negative control, expression of GFP displayed no significant effect indicating that expression of an exogenous protein was unable to perturb hepcidin expression (Fig. 3*C*). Surprisingly, R325A-fHjv exhibited a similar extent of induction of hepcidin expression as fHjv (Fig. 3*C*). This is in contrast to our initial prediction that abolishment of furin-cleaved Hjv in the serum would enhance hepcidin expression by increasing BMP6 signaling in the liver. In comparison with GFP, expression of both fHjv and R325A-fHjv increased hepatic mRNA of Id1 to a similar extent (Fig. 3*F*). Neither induced the expression of the inflammation factors, IL-6 and Activin-B, in the liver (supplemental Fig. S3, *C* and *D*). These results provided further evidence to support that fHjv induces hepcidin expression specifically through the BMP signaling pathway. As expected, the increased hepcidin mRNA observed with fHjv and R325A-fHjv reduced serum iron to a similar extent (Fig. 3*B*). No further decrease in the liver non-heme iron was detected because these animals were fed an ID diet (Fig. 3*A*). Together, these observations indicate that serum Hjv derived from the liver does not repress the ability of membrane-anchored Hjv to induce hepcidin expression *in vivo*.

Role of HJV-Neogenin Interaction in the Liver

Disruption of the Predominant MT2 Cleavage Site in Hjv Abolishes Hjv-Neogenin Interaction and Reduces the Induction of Hepcidin mRNA in Vivo—Neogenin also interacts with MT2 to facilitate MT2 cleavage of HJV in cultured cells (20). MT2 cleaves HJV at distinct sites from furin (24). The major MT2 cleavage site was mapped to Arg-288 in HJV (corresponding to Arg-281 for murine Hjv), and the R288A mutation in HJV abolishes MT2 cleavage in transfected cells (24). Because mutations of the *MT2* gene in humans or deletion of the catalytic domain of MT2 in mice result in inappropriately high hepcidin expression and iron deficiency (25, 39), we hypothesized that disruption of the MT2 cleavage site in Hjv would increase its induction of hepcidin expression *in vivo*. To test this hypothesis, we first examined whether MT2 cleaves Hjv in the liver. Surprisingly, no predicted MT2-cleaved fHjv band was detected in the serum of $Hjv^{-/-}$ mice expressing fHjv, A183R-fHjv, G313V-fHjv, or R325A-fHjv (Figs. 3*E*, and 4, *A* and *B*). When compared with fHjv, expression of R281A-fHjv that is expected to be resistant to MT2 cleavage in the liver of $Hjv^{-/-}$ mice did not reduce the intensities of serum fHjv bands (Fig. 3*E*, *lower panel*, *lanes 11*/12 *versus 3*/*4*, supplemental Fig. S3*E*). These results further support that the fHjv detected in serum was a product of furin cleavage. On the basis of these observations, we predict that lack of detectable MT2-cleaved fHjv in the serum might be due to its level falling below the limit of detection because of a rapid clearance from the circulation.

To gain indirect evidence for MT2 cleavage of fHjv *in vivo*, mice that express fHjv, R325A-fHjv, or R281A-fHjv were intraperitoneally injected with aprotinin, a serine protease inhibitor, at ~80 mg/kg body weight 3 times (4, 16, and 24 h before euthanization), to inhibit the enzymatic activity of MT2. The dosage of aprotinin was estimated on the basis of studies in HepG2 cells. HepG2 cells endogenously express both furin and MT2 mRNA (24). Expression of HJV in HepG2 cells led to a detection of two major soluble forms of HJV in the conditioned medium by Western blot using an antibody against the entire HJV extracellular domain (supplemental Fig. S4, *middle, lanes 1–3*). The *upper band* represented the furin cleavage product that was blocked by the furin convertase inhibitor in our previous studies (24), and the *lower band* was the MT2 cleavage products that was inhibited by aprotinin (supplemental Fig. S4, *middle panel*). Inhibition of MT2 cleavage of HJV by aprotinin was concomitantly associated with an increase in the intensity of furin-cleaved HJV bands (supplemental Fig. S4, *lower panel*), suggesting that aprotinin did not affect the enzymatic activity of furin. If MT2 cleaves Hjv *in vivo*, inhibition of MT2 activity by aprotinin in these mice is predicted to increase the furin-cleaved fHjv in the serum. Interestingly, administration of aprotinin increased serum fHjv levels by a similar extent for both fHjv and R281A-fHjv mice (Fig. 3*E*, *lanes 3*/*4 versus 5*/*6* and *11*/*12 versus 13*/*14*, supplemental Fig. S3*E*). The lack of detectable serum fHjv in R325A-fHjv mice was due to the disruption of furin cleavage site. These results indirectly indicate that MT2 cleaves Hjv in the liver and that Arg-281 in Hjv might not be the only MT2 cleavage site *in vivo*.

The induction of hepcidin mRNA by R281A-fHjv was next examined in the liver of $Hjv^{-/-}$ mice. In contrast to our prediction that expression of R281A-fHjv that is resistant to MT2 cleavage would increase hepcidin expression, qRT-PCR analysis revealed an attenuated induction when compared with fHjv (Fig. 3*C* and supplemental Fig. S3*F*). This reduced hepcidin mRNA was correlated with a compromised induction of BMP signaling as manifested by significantly lower levels of Id1 mRNA than the fHjv group in the liver (Fig. 3*F*). Consistent with reduced hepcidin expression, serum iron levels in R281A-fHjv mice were significantly higher than that of fHjv mice (Fig. 3*B*). This unexpected finding is in agreement with a clinical study, which shows that R288W mutation in human HJV (corresponding to R281W in murine Hjv) causes JH (40). R288A-HJV traffics to the plasma membrane (24), indicating that it is folded correctly. To explore the potential mechanism, we determined whether this mutation affects its interaction with other important proteins. Similar to wild-type HJV, R288A-HJV was co-immunoprecipitated with both TfR2 and fHFE (Fig. 5*A*). Intriguingly, both R281A-fHjv and R288A-HJV had reduced interaction with neogenin in transfected HEK293 cells by immunoprecipitation (Fig. 5, *B* and *C*). These observations indicate that R288A mutation in HJV disrupts its association with neogenin, but not with TfR2 or HFE, and suggest that the attenuated induction of hepcidin expression by R281A-fHjv in $Hjv^{-/-}$ mice results from a lack of interaction with neogenin. These findings provided another line of evidence supporting the critical role of neogenin in the induction of hepcidin by HJV.

Neogenin Interacts with ALK3 through Its Ig Domains—Because the interaction of HJV with neogenin was critical for the induction of hepcidin expression through the BMP signaling pathway *in vivo*, we wanted to investigate whether neogenin itself had any direct interactions with the BMP receptors, and whether these interactions occurred through domains other than FNIII 5–6 in neogenin (Fig. 6*A*). FNIII 5–6 subdomains are responsible for interaction with HJV (15). Human liver expresses two type-I BMP receptors, ALK2 and ALK3 (41). Both ALK3 and (to a lesser extent) ALK2 are essential for hepcidin expression in mice (12). We examined the interaction of neogenin with ALK2 and ALK3 by immunoprecipitation. HEK293 cells that stably express ALK2 with a HA tag (ALK2/HA) or ALK3 with a HA tag (ALK3/HA) were transfected with neogenin. Interestingly, rabbit anti-neogenin antibody was able to pull down ALK3/HA, but not ALK2/HA (Fig. 6, *B* and *C*). These observations indicate that neogenin interacts with ALK3.

To map the domains in neogenin responsible for this interaction, a truncated construct without all four Ig subdomains but with an intact signal peptide sequence (neogenin/ΔIg; Fig. 6*A*) was generated. Deletion of four Ig subdomains did not affect its trafficking to the plasma membrane in HEK293 cells (Fig. 6*D*). An anti-neogenin antibody was able to pulldown neogenin/ΔIg. But no detectable ALK3/HA was co-immunoprecipitated with neogenin/ΔIg (Fig. 6*C*). These observations suggest that neogenin interacts with ALK3 through its Ig domains, which is a different region than what binds HJV, implying that these interactions may not be mutually exclusive. These findings also provide a potential mechanism for the involvement of neogenin in the BMP signaling pathway through binding to ALK3.

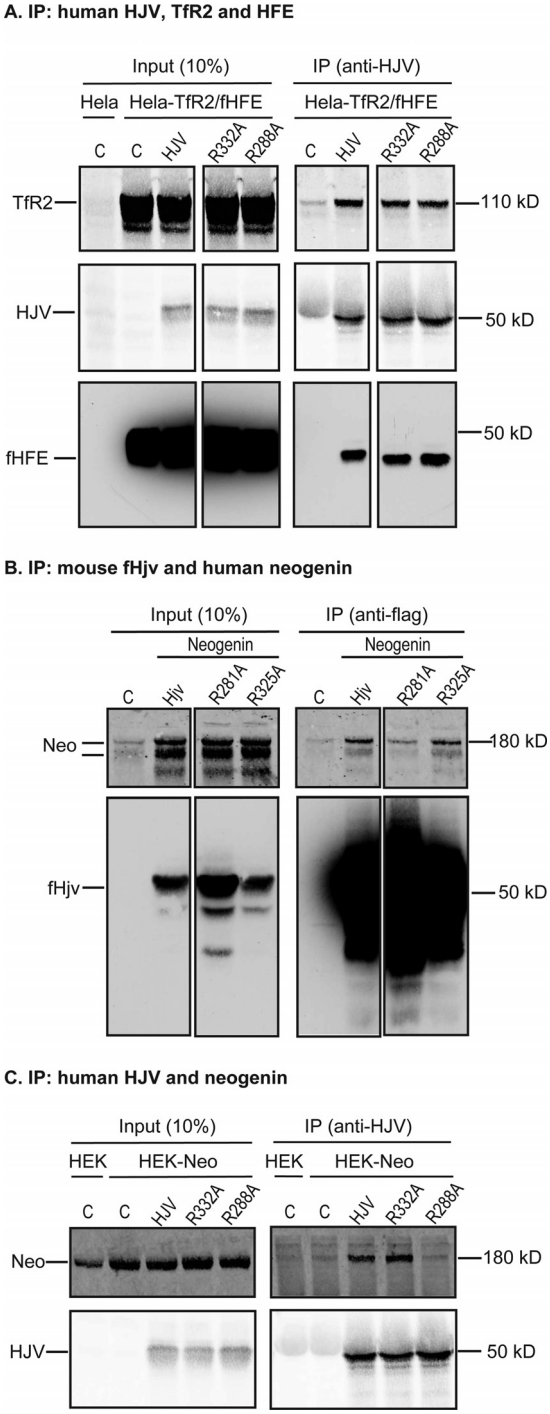

FIGURE 5. **R288A mutation in HJV and R281A mutation in Hjv disrupt the interaction with neogenin, but not with HFE or TfR2.** *A,* co-immunoprecipitation of WT, R332A, and R288A-HJV with HFE and TfR2. HeLa-TfR2/fHFE cells were transfected by pcDNA3 (*C*), pcDNA3-HJV, R332A-HJV, and R288A-HJV, immunoprecipitated (*IP*) by using anti-HJV antibody, and immunodetected for TfR2, HJV, and fHFE. The entire images are illustrated in supplemental Fig. S1C. *B,* co-immunoprecipitation of WT, R281A, and R325A-fHjv with neogenin. HEK293 cells were co-transfected by pcDNA3-neogenin with pCMV9-fHjv, R281A-fHjv, or R325A-fHjv, immunoprecipitated by using anti-FLAG M2 beads, and immunodetected for neogenin (*Neo*) and fHjv. HEK293 cells transfected with pCMV9 alone pCMV9 (*C*) were included as a control. The entire images are illustrated in supplemental Fig. S1A. *C,* co-immunoprecipitation of WT, R332A, and R288A-HJV with neogenin. HEK293-neogenin (HEK-Neo) cells were transfected by pcDNA3 (*C*), pcDNA3-HJV, R332A-HJV, and R288A-HJV, immunoprecipitated by using anti-HJV antibody, and immunodetected for neogenin (Neo) and HJV. HEK293 cells (HEK) were included as a control. All experiments were repeated at least three times with consistent results.

Disruption of Hjv Interaction with BMP Ligand, but Not Neogenin, also Reduces the Induction of Hepcidin mRNA in the Liver—Because HJV can simultaneously bind BMP2 and neogenin (13) and the above studies showed that the Hjv-neogenin interaction is essential for hepcidin expression, we next wanted to validate the importance of BMP-HJV interactions in HJV induction of hepcidin expression *in vivo*. The crystallographic studies indicate that the G99V mutation in HJV causes JH in humans (40). The Gly-99 residue in HJV (corresponding to Gly-92 in mouse Hjv) is located at the interface with BMP2 (13). In transfected cells, G92V mutation in Hjv abolishes the binding to BMP2 (33). Immunoprecipitation analysis indicated that the G99V mutation in HJV did not affect its interaction with neogenin, TfR2, or HFE (Fig. 7, *A* and *B*). Thus the major defect of G99V-HJV or G92V-Hjv is a lack of interaction with BMP.

G92V-Hjv with no tag was expressed in the liver of $Hjv^{-/-}$ mice by using AAV8. Expression of wild-type Hjv mRNA at ~15% of the levels seen in the wild-type mice was able to restore hepcidin expression in $Hjv^{-/-}$ mice (Fig. 7, *C* and *D*) (31). This suggests that the levels of Hjv in the liver is not a limiting factor for the induction of hepcidin expression (31). Interestingly, expression of a similar level of G92V-Hjv mRNA was only able to induce hepcidin mRNA to 20% of that induced by wild-type Hjv, with no evident increase in pSmad in the liver (Fig. 7, *C–F*). In this study, we did not detect the levels of expressed Hjv protein because of lack of an appropriate antibody for immunodetection of the liver Hjv. These results indicate that the attenuated induction of hepcidin mRNA by G92V-Hjv resulted from a lack of activation of the BMP signaling. Consistent with low hepcidin mRNA, no significant reduction of serum iron or liver non-heme iron was detected in the G92V-Hjv group (Fig. 7, *G* and *H*). These results recapitulated the low hepcidin status in JH patients with G99V-HJV and substantiated the pivotal role of HJV-BMP interaction for HJV induction of hepcidin mRNA in the liver.

Discussion

This study investigated the role of the Hjv-neogenin interaction in the liver of $Hjv^{-/-}$ mice. Our results showed that this interaction is essential for the efficient induction of hepcidin mRNA by Hjv through the BMP signaling pathway. This process likely involves the association of neogenin with ALK3. In contrast to the observations in cultured cells, additional studies revealed that the Hjv-neogenin interaction was not required for furin cleavage of Hjv in the liver, and that the furin-cleaved soluble Hjv from the liver did not affect hepcidin expression. Further studies also substantiated the pivotal role of Hjv-BMP interaction in hepcidin expression. These findings support the key role of neogenin in the assembly of an HJV·BMP·BMP receptor complex to induce BMP signaling and hepcidin expression in the liver.

We established a mouse model to study the function of neogenin in Hjv induction of hepcidin expression in the liver by using AAV8 with a liver-specific promoter, FLAG-tagged Hjv, and adult $Hjv^{-/-}$ mice. This AAV8 vector was able to specifically deliver Hjv cDNA into the liver of mice (31) with no activation of inflammation at a wide range of dosage. Addition of a FLAG tag to Hjv did not affect Hjv induction of the BMP sig-

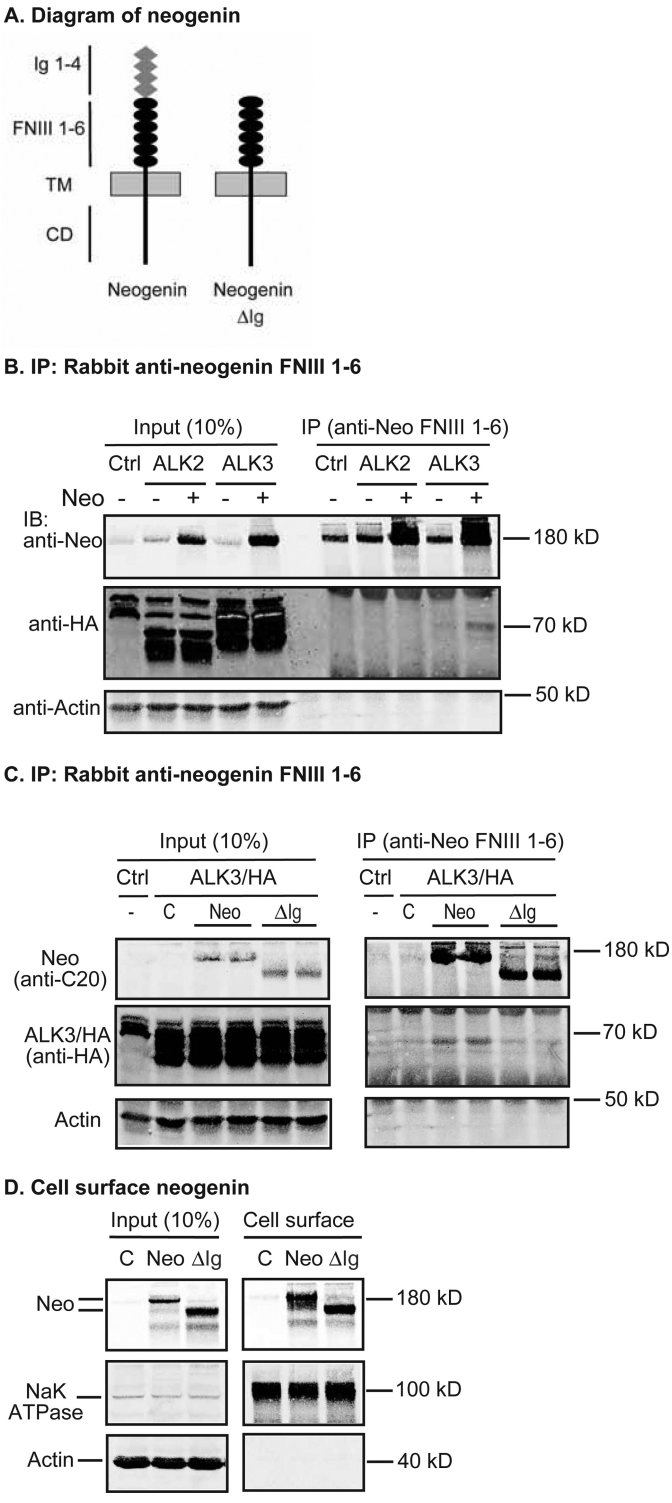

FIGURE 6. **Neogenin is co-immunoprecipitated with ALK3 through its Ig domains.** *A,* diagrams of neogenin and truncated neogenin lacking Ig domains (neogenin ΔIg). *TM*, transmembrane domain; *CD*, cytoplasmic domain. *B,* anti-neogenin FNIII 1–6 antibody pulled down neogenin with ALK3/HA, but not ALK2/HA. HEK293-ALK2/HA or ALK3/HA cells were transfected with pcDNA3 (−) or pcDNA3-neogenin plasmid DNA (+), immunoprecipitated (*IP*) by using rabbit anti-neogenin FNIII 1–6 antibody, and immunoblotted (*IB*) with goat anti-neogenin (*Neo*), mouse anti-HA, or mouse anti-β actin antibodies in lysate input (*Input*) and IP eluate. *C,* neogenin ΔIg was not co-immunoprecipitated with ALK3/HA by anti-neogenin FNIII 1–6 antibody. HEK293-ALK3/HA cells were transfected with pcDNA3 (*C*), pcDNA3-neogenin, or neogenin ΔIg (ΔIg) plasmid DNA, immunoprecipitated by using rabbit anti-neogenin FNIII 1–6 antibody, and immunodetected for neogenin, ALK3/HA, and β-actin. *D,* biotinylation of cell surface neogenin. HEK293 cells were transfected with pcDNA3 (*C*), pcDNA3-neogenin, or neogenin ΔIg (ΔIg) plasmid DNA, followed by biotinylation of cell surface proteins at 4 °C and immunodetection of neogenin, Na^+/K^+-ATPase, and β-actin in the biotinylated proteins (*Cell surface*) and cell lysate input. All experiments were repeated at least three times with consistent results.

naling and hepcidin mRNA. Rather it allowed detection of the fHjv protein in the liver and furin-cleaved fHjv in the serum. The use of adult mice circumvented the confounding issues of developmental defects encountered in neogenin mutant mice (18). In the studies of A183R and G313V-fHjv, results revealed a positive correlation between the administered AAV8 particles and the expressed Hjv at both mRNA and protein levels. Thus this model allows an easy control of the expression levels of Hjv simply by adjusting the dosage of AAV8.

The first line of evidence to support the critical role of HJV-neogenin interaction in Hjv induction of hepcidin expression was derived from the studies of A183R-fHjv that did not interact with neogenin. This mutant was generated based on co-crystal studies of RGMb and neogenin FNIII 5–6 domains (14). In the liver of $Hjv^{-/-}$ mice, expression of A183R-fHjv exhibited an attenuated BMP signaling and a reduced hepcidin mRNA. The extent of reduction was similar to G313V-fHjv that also did not interact with neogenin. G313V mutation in Hjv that corresponds to mutations in human HJV, is a disease-causing mutation (2). Our results ruled out the possibilities that these mutations had a major effect on Hjv localization on the plasma membrane and its interaction with TfR2 and HFE. Although one study reported an accumulation of overexpressed G320V-HJV in the endoplasmic reticulum compartments of transfected cells by EM analysis (32), another study showed no effect of G313V mutation on Hjv trafficking onto the plasma membrane by biotinylation of cell surface proteins (33). Neither mutation resides within the N-terminal portion of HJV that is responsible for HJV binding to BMP (13). Therefore, it is unlikely that the attenuated induction of hepcidin expression by these mutations resulted from the reduced binding to BMPs. Thus the major defect is that these mutations disrupt the Hjv-neogenin interaction. These observations indicate that the interaction with neogenin is essential for Hjv-mediated induction of hepcidin expression through the BMP signaling in the liver. The lack of complete abolishment of hepcidin expression by these mutations might be due to the possibility that they still interact with neogenin with low affinity.

The second line of evidence supporting the role of the neogenin-HJV interaction in the regulation of iron homeostasis was obtained from studying MT2 cleavage of Hjv. Arg-281 in Hjv is expected to be the major MT2 cleavage site from the studies in transfected cells (24). We initially predicted that disruption of MT2 cleavage of Hjv by the R281A mutation would lead to a greater induction of hepcidin expression than wild-type fHjv, because mutations of the *MT2* gene in humans or deletion of the catalytic domain of MT2 in mice result in an inappropriately high hepcidin expression (25, 39). Unexpectedly, expression of R281A-fHjv in the liver of $Hjv^{-/-}$ mice revealed a greatly reduced induction of hepcidin expression when compared with wild-type fHjv. The extent of reduction is comparable with A183R- and G313V-fHjv. This unanticipated

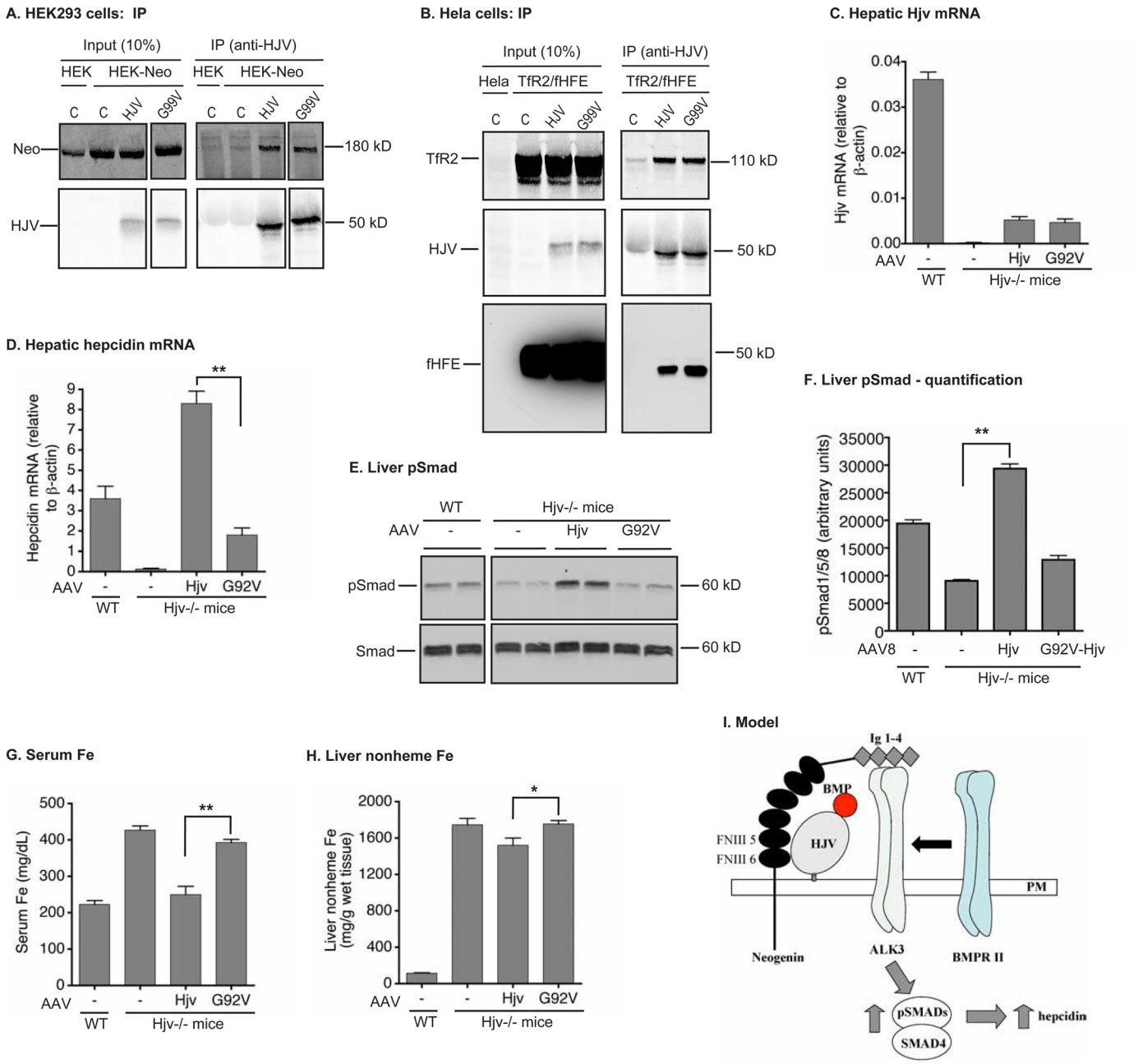

FIGURE 7. **G99V-HJV was co-immunoprecipitated with neogenin, HFE, and TfR2 in transfected cells, and G92V-Hjv had a reduced capability to induce the BMP signaling and hepcidin expression in Hjv$^{-/-}$ mice.** *A,* co-immunoprecipitation (*IP*) of WT and G99V-HJV with neogenin. HEK293-neogenin (HEK-Neo) were transfected by pcDNA3 (*C*), pcDNA3-HJV, and G99V-HJV, immunoprecipitated by using anti-HJV antibody, and immunodetected for neogenin (*Neo*) and HJV. HEK293 cells (*HEK*) were included as a control. The entire images are illustrated in supplemental Fig. S1*B*. *B,* co-immunoprecipitation of WT and G99V-HJV with HFE and TfR2. HeLa-TfR2/fHFE cells were transfected by pcDNA3 (*C*), pcDNA3-HJV, and G99V-HJV, immunoprecipitated by using anti-HJV antibody, and immunodetected for TfR2, HJV, and fHFE. All immunoprecipitation experiments were repeated at least three times with consistent results. *C* and *D,* RT-PCR analysis of Hjv and hepcidin mRNA in the liver. Results are expressed as the amount relative to that of β-actin for each sample. The mean $\pm$ S.D. are presented. *E,* Western blot analysis of pSmad and Smad in 250 μg of liver tissue proteins. *F,* quantification of pSmad bands in the Western blot images of liver extracts by Licor. *G,* serum iron analysis. *H,* liver nonheme iron analysis. $n = 5$ for each group. *, $p < 0.05$; **, $p < 0.01$. *I,* model for neogenin induction of hepcidin expression by simultaneous binding to HJV and ALK3 through FNIII 5–6 domains and Ig 1–4 domains, respectively.

finding was supported by a clinical study, which shows that the R288W mutation in human HJV (corresponding to R281W in murine Hjv) causes JH (40). This implies that Arg-281 in Hjv acts as a key residue for its function. Further studies indicate that the R281A mutation in Hjv disrupted its interaction with neogenin, but not with TfR2 or HFE, which is similar to A183R- and G313V-fHjv. These findings strengthen the idea that the HJV-neogenin interaction is essential for hepcidin expression. Additionally, we also obtained indirect evidence showing that MT2 did cleave Hjv in the liver and that Arg-281 might not be the only MT2 cleavage site in Hjv.

Previous studies indicate that neogenin is also involved in furin cleavage of HJV. In HepG2 cells, secretion of furin-cleaved HJV is blocked by siRNA knockdown of endogenous neogenin (19, 20). In HEK293 cells and cultured primary mouse muscles, expression of neogenin inhibits HJV secretion (18). In this

study, we confirmed that furin cleavage of Hjv in the liver used the same site as in transfected cells (21, 23, 24). Furin-cleaved fHjv in the serum was detectable by Western blot, which indicates that the liver is a source of serum Hjv. Interestingly, when compared with fHjv, there was no evident decrease of furin-cleaved fHjv in the serum of mice expressing A183R-fHjv or R281A-fHjv that did not interact with neogenin. These data indicate that HJV-neogenin interaction may not be required for furin cleavage of HJV in the liver, which is contrary to the previous observations in transfected cells. However, this does not rule out the possibility that neogenin is involved in furin cleavage of HJV in other tissues.

Furin cleaved-soluble HJV is proposed to be a negative regulator of hepatic hepcidin expression by acting as a decoy that competes with membrane HJV for binding to BMP6. In this study, abolishment of furin cleavage of Hjv in the liver (by expressing R325A-fHjv) resulted in no detectable fHjv in the serum, but had no evident effect on hepcidin mRNA. Thus soluble Hjv does not appear to be in sufficient amounts to compete with membrane-bound Hjv for binding to BMPs. It is likely that furin cleavage of Hjv represents a process of membrane Hjv turnover *in vivo*. In HepG2 cells, membrane HJV has a half-life of about 1 h, and HJV release from the cells constitutes the major pathway of HJV turnover (42).

Mechanistic studies indicate that neogenin interacts with ALK3 through its Ig subdomains, which provides a potential linkage of neogenin to the BMP signaling. ALK3 is an important type-I BMP receptor in the liver for BMP signaling and hepcidin expression in mice (12). Thus neogenin can simultaneously bind both HJV and ALK3 via its FNIII 5–6 subdomains that are immediately adjacent to the transmembrane domain and its N-terminal Ig domains, respectively. This study also validated the essential role of Hjv-BMP interaction for induction of hepcidin expression by using G92V-Hjv that interacts with neogenin but does not bind to BMP2 (33). Structural analysis indicates that the N-terminal portion of Hjv shares an overlapping BMP2-binding surface with the ectodomain of ALK3 (13).

On the basis of the observations in this and previous studies, we propose a model in which neogenin acts as a scaffold by a direct association with both HJV and ALK3 to facilitate the assembly of BMP ligand·ALK3·type-II BMP receptor complex in the liver, which subsequently initiates the BMP signaling cascade to induce the transcription of the hepcidin gene (Fig. 7*I*). Consistent with this model, mutations in HJV that disrupt its interaction with either neogenin or BMP cause JH. In summary, this study provided evidence in support of the idea that HJV induction of hepcidin expression in the liver requires its association with both neogenin and BMP.

Author Contributions—N. Z., J. E. M., C. A. E., and A. Z. designed the experiments, analyzed the data, and wrote the paper. N. Z., J. E. M., R. H. Z., M. W., and A. Z. performed the experiments.

Acknowledgments—We thank Dr. Jodie Babitt and Dr. Herbert Lin for fHJV-pCMV9, Dr. Eric R. Fearon for Neogenin-pcDNA3.1, Dr. Peter ten Dijke for pcDNA3-ALK2-HA and ALK3-HA, and Dr. Nancy Andrews for Hjv$^{-/-}$ mice.

References

1. Matsunaga, E., and Chédotal, A. (2004) Repulsive guidance molecule/neogenin: a novel ligand-receptor system playing multiple roles in neural development. *Dev. Growth Differ.* **46,** 481–486
2. Papanikolaou, G., Samuels, M. E., Ludwig, E. H., MacDonald, M. L., Franchini, P. L., Dubé, M. P., Andres, L., MacFarlane, J., Sakellaropoulos, N., Politou, M., Nemeth, E., Thompson, J., Risler, J. K., Zaborowska, C., Babakaiff, R., *et al.* (2004) Mutations in HFE2 cause iron overload in chromosome 1q-linked juvenile hemochromatosis. *Nat. Genet.* **36,** 77–82
3. Nemeth, E., Tuttle, M. S., Powelson, J., Vaughn, M. B., Donovan, A., Ward, D. M., Ganz, T., and Kaplan, J. (2004) Hepcidin regulates cellular iron efflux by binding to ferroportin and inducing its internalization. *Science* **306,** 2090–2093
4. Valore, E. V., and Ganz, T. (2008) Posttranslational processing of hepcidin in human hepatocytes is mediated by the prohormone convertase furin. *Blood Cells Mol. Dis.* **40,** 132–138
5. Niederkofler, V., Salie, R., and Arber, S. (2005) Hemojuvelin is essential for dietary iron sensing, and its mutation leads to severe iron overload. *J. Clin. Invest.* **115,** 2180–2186
6. Huang, F. W., Pinkus, J. L., Pinkus, G. S., Fleming, M. D., and Andrews, N. C. (2005) A mouse model of juvenile hemochromatosis. *J. Clin. Invest.* **115,** 2187–2191
7. Chen, W., Huang, F. W., de Renshaw, T. B., and Andrews, N. C. (2011) Skeletal muscle hemojuvelin is dispensable for systemic iron homeostasis. *Blood* **117,** 6319–6325
8. Gkouvatsos, K., Wagner, J., Papanikolaou, G., Sebastiani, G., and Pantopoulos, K. (2011) Conditional disruption of mouse HFE2 gene: maintenance of systemic iron homeostasis requires hepatic but not skeletal muscle hemojuvelin. *Hepatology* **54,** 1800–1807
9. Babitt, J. L., Huang, F. W., Wrighting, D. M., Xia, Y., Sidis, Y., Samad, T. A., Campagna, J. A., Chung, R. T., Schneyer, A. L., Woolf, C. J., Andrews, N. C., and Lin, H. Y. (2006) Bone morphogenetic protein signaling by hemojuvelin regulates hepcidin expression. *Nat. Genet.* **38,** 531–539
10. Andriopoulos, B., Jr., Corradini, E., Xia, Y., Faasse, S. A., Chen, S., Grgurevic, L., Knutson, M. D., Pietrangelo, A., Vukicevic, S., Lin, H. Y., and Babitt, J. L. (2009) BMP6 is a key endogenous regulator of hepcidin expression and iron metabolism. *Nat. Genet.* **41,** 482–487
11. Meynard, D., Kautz, L., Darnaud, V., Canonne-Hergaux, F., Coppin, H., and Roth, M. P. (2009) Lack of the bone morphogenetic protein BMP6 induces massive iron overload. *Nat. Genet.* **41,** 478–481
12. Steinbicker, A. U., Bartnikas, T. B., Lohmeyer, L. K., Leyton, P., Mayeur, C., Kao, S. M., Pappas, A. E., Peterson, R. T., Bloch, D. B., Yu, P. B., Fleming, M. D., and Bloch, K. D. (2011) Perturbation of hepcidin expression by BMP type I receptor deletion induces iron overload in mice. *Blood* **118,** 4224–4230
13. Healey, E. G., Bishop, B., Elegheert, J., Bell, C. H., Padilla-Parra, S., and Siebold, C. (2015) Repulsive guidance molecule is a structural bridge between neogenin and bone morphogenetic protein. *Nat. Struct. Mol. Biol.* **22,** 458–465
14. Bell, C. H., Healey, E., van Erp, S., Bishop, B., Tang, C., Gilbert, R. J., Aricescu, A. R., Pasterkamp, R. J., and Siebold, C. (2013) Structure of the repulsive guidance molecule (RGM)-neogenin signaling hub. *Science* **341,** 77–80
15. Yang, F., West, A. P., Jr., Allendorph, G. P., Choe, S., and Bjorkman, P. J. (2008) Neogenin interacts with hemojuvelin through its two membrane-proximal fibronectin type III domains. *Biochemistry* **47,** 4237–4245
16. Zhang, A. S., Yang, F., Wang, J., Tsukamoto, H., and Enns, C. A. (2009) Hemojuvelin-neogenin interaction is required for bone morphogenic protein-4-induced hepcidin expression. *J. Biol. Chem.* **284,** 22580–22589
17. Zhang, A. S., West, A. P., Jr., Wyman, A. E., Bjorkman, P. J., and Enns, C. A. (2005) Interaction of hemojuvelin with neogenin results in iron accumulation in human embryonic kidney 293 cells. *J. Biol. Chem.* **280,** 33885–33894
18. Lee, D. H., Lee, D. H., Zhou, L. J., Zhou, L. J., Zhou, Z., Xie, J. X., Xie, J. X., Jung, J. U., Liu, Y., Xi, C. X., Mei, L., and Xiong, W. C. (2010) Neogenin inhibits HJV secretion and regulates BMP-induced hepcidin expression and iron homeostasis. *Blood* **115,** 3136–3145

19. Zhang, A. S., Yang, F., Meyer, K., Hernandez, C., Chapman-Arvedson, T., Bjorkman, P. J., and Enns, C. A. (2008) Neogenin-mediated hemojuvelin shedding occurs after hemojuvelin traffics to the plamsa membrane. *J. Biol. Chem.* **283,** 17494–17502
20. Enns, C. A., Ahmed, R., and Zhang, A. S. (2012) Neogenin interacts with matriptase-2 to facilitate hemojuvelin cleavage. *J. Biol. Chem.* **287,** 35104–35117
21. Silvestri, L., Pagani, A., and Camaschella, C. (2008) Furin mediated release of soluble hemojuvelin: a new link between hypoxia and iron homeostasis. *Blood* **111,** 924–931
22. Silvestri, L., Pagani, A., Nai, A., De Domenico, I., Kaplan, J., and Camaschella, C. (2008) The serine protease matriptase-2 (TMPRSS6) inhibits hepcidin activation by cleaving membrane hemojuvelin. *Cell Metab.* **8,** 502–511
23. Lin, L., Nemeth, E., Goodnough, J. B., Thapa, D. R., Gabayan, V., and Ganz, T. (2008) Soluble hemojuvelin is released by proprotein convertase-mediated cleavage at a conserved polybasic RNRR site. *Blood Cells Mol. Dis.* **40,** 122–131
24. Maxson, J. E., Chen, J., Enns, C. A., and Zhang, A. S. (2010) Matriptase-2- and proprotein convertase-cleaved forms of hemojuvelin have different roles in the down-regulation of hepcidin expression. *J. Biol. Chem.* **285,** 39021–39028
25. Du, X., She, E., Gelbart, T., Truksa, J., Lee, P., Xia, Y., Khovananth, K., Mudd, S., Mann, N., Moresco, E. M., Beutler, E., and Beutler, B. (2008) The serine protease TMPRSS6 is required to sense iron deficiency. *Science* **320,** 1088–1092
26. Finberg, K. E., Whittlesey, R. L., Fleming, M. D., and Andrews, N. C. (2010) Downregulation of Bmp/Smad signaling by Tmprss6 is required for maintenance of systemic iron homeostasis. *Blood* **115,** 3817–3826
27. Lin, L., Goldberg, Y. P., and Ganz, T. (2005) Competitive regulation of hepcidin mRNA by soluble and cell-associated hemojuvelin. *Blood* **106,** 2884–2889
28. Zhang, A. S., Anderson, S. A., Meyers, K. R., Hernandez, C., Eisenstein, R. S., and Enns, C. A. (2007) Evidence that inhibition of hemojuvelin shedding in response to iron is mediated through neogenin. *J. Biol. Chem.* **282,** 12547–12556
29. D'Alessio, F., Hentze, M. W., and Muckenthaler, M. U. (2012) The hemochromatosis proteins HFE, TfR2, and HJV form a membrane-associated protein complex for hepcidin regulation. *J. Hepatol.* **57,** 1052–1060
30. Latour, C., Besson-Fournier, C., Meynard, D., Silvestri, L., Gourbeyre, O., Aguilar-Martinez, P., Schmidt, P. J., Fleming, M. D., Roth, M. P., and Coppin, H. (2016) Differing impact of the deletion of hemochromatosis-associated molecules HFE and TFR2 on the iron phenotype of mice lacking BMP6 or HJV. *Hepatology* **63,** 126–137
31. Zhang, A. S., Gao, J., Koeberl, D. D., and Enns, C. A. (2010) The role of hepatocyte hemojuvelin in the regulation of bone morphogenic protein-6 and hepcidin expression *in vivo*. *J. Biol. Chem.* **285,** 16416–16423
32. Silvestri, L., Pagani, A., Fazi, C., Gerardi, G., Levi, S., Arosio, P., and Camaschella, C. (2007) Defective targeting of hemojuvelin to plasma membrane is a common pathogenetic mechanism in juvenile hemochromatosis. *Blood* **109,** 4503–4510
33. Kuns-Hashimoto, R., Kuninger, D., Nili, M., and Rotwein, P. (2008) Selective binding of RGMc/hemojuvelin, a key protein in systemic iron metabolism, to BMP-2 and neogenin. *Am. J. Physiol. Cell Physiol.* **294,** C994–C1003
34. Gutschow, P., Schmidt, P. J., Han, H., Ostland, V., Bartnikas, T. B., Pettiglio, M. A., Herrera, C., Butler, J. S., Nemeth, E., Ganz, T., Fleming, M. D., and Westerman, M. (2015) A competitive enzyme-linked immunosorbent assay specific for murine hepcidin-1: correlation with hepatic mRNA expression in established and novel models of dysregulated iron homeostasis. *Haematologica* **100,** 167–177
35. Lefebvre, T., Dessendier, N., Houamel, D., Ialy-Radio, N., Kannengiesser, C., Manceau, H., Beaumont, C., Nicolas, G., Gouya, L., Puy, H., and Karim, Z. (2015) LC-MS/MS method for hepcidin-25 measurement in human and mouse serum: clinical and research implications in iron disorders. *Clin. Chem. Lab. Med.* **53,** 1557–1567
36. Nai, A., Rubio, A., Campanella, A., Gourbeyre, O., Artuso, I., Bordini, J., Gineste, A., Latour, C., Besson-Fournier, C., Lin, H. Y., Coppin, H., Roth, M. P., Camaschella, C., Silvestri, L., and Meynard, D. (2016) Limiting hepatic Bmp-Smad signaling by matriptase-2 is required for erythropoietin-mediated hepcidin suppression in mice. *Blood,* 10.1182/blood-2015-11-681494
37. Besson-Fournier, C., Latour, C., Kautz, L., Bertrand, J., Ganz, T., Roth, M. P., and Coppin, H. (2012) Induction of activin B by inflammatory stimuli up-regulates expression of the iron-regulatory peptide hepcidin through Smad1/5/8 signaling. *Blood* **120,** 431–439
38. Kautz, L., Meynard, D., Monnier, A., Darnaud, V., Bouvet, R., Wang, R. H., Deng, C., Vaulont, S., Mosser, J., Coppin, H., and Roth, M. P. (2008) Iron regulates phosphorylation of Smad1/5/8 and gene expression of Bmp6, Smad7, Id1, and Atoh8 in the mouse liver. *Blood* **112,** 1503–1509
39. Finberg, K. E., Heeney, M. M., Campagna, D. R., Aydinok, Y., Pearson, H. A., Hartman, K. R., Mayo, M. M., Samuel, S. M., Strouse, J. J., Markianos, K., Andrews, N. C., and Fleming, M. D. (2008) Mutations in TMPRSS6 cause iron-refractory iron deficiency anemia (IRIDA). *Nat. Genet.* **40,** 569–571
40. Lanzara, C., Roetto, A., Daraio, F., Rivard, S., Ficarella, R., Simard, H., Cox, T. M., Cazzola, M., Piperno, A., Gimenez-Roqueplo, A. P., Grammatico, P., Volinia, S., Gasparini, P., and Camaschella, C. (2004) Spectrum of hemojuvelin gene mutations in 1q-linked juvenile hemochromatosis. *Blood* **103,** 4317–4321
41. Xia, Y., Babitt, J. L., Sidis, Y., Chung, R. T., and Lin, H. Y. (2008) Hemojuvelin regulates hepcidin expression via a selective subset of BMP ligands and receptors independently of neogenin. *Blood* **111,** 5195–5204
42. Maxson, J. E., Enns, C. A., and Zhang, A. S. (2009) Processing of hemojuvelin requires retrograde trafficking to the Golgi in HepG2 cells. *Blood* **113,** 1786–1793